Unstable behaviour of normally-off GaN E-HEMT under short-circuit

P. J. Martínez, E. Maset, E. Sanchis-Kilders, V. Esteve, J. Jordán, J. Bta. Ejea and A. Ferreres

University of Valencia, Department of Electronic Engineering, 46100 Burjassot, Spain

Enrique.maset@uv.es

Abstract. The short-circuit withstand capability of the power switching devices plays an important role in fault detection and protection of power circuits. In this work, an experimental study on short-circuit (SC) capability of commercial 600 V Gallium Nitride Enhancement-mode High-Electron-Mobility transistors (E-HEMT) is presented. A different failure mechanism has been identified for commercial p-doped GaN gate (p-GaN) HEMT and metal-insulator-semiconductor (MIS) HEMT. Additionally, to the well know thermal breakdown, a premature breakdown is shown on both GaN HEMTs, triggered by hot electron trapping at the surface, which denote that current commercial GaN HEMTs need efforts for improving SC ruggedness.

1. Introduction

Wide Bandgap (WBG) semiconductors like silicon carbide (SiC) and gallium nitride (GaN) offer, among others, higher electro thermal performance, which makes them very attractive for industrial applications and it is expected that they become the best choice to replace silicon technology in the near future [1-3]. The advantages of WBG semiconductors at system level are: low conduction and switching losses, high temperature capability and high thermal conductivity. In 2001, the first commercial wide bandgap power device, a Silicon Carbide (SiC) Schottky-diode became commercially available and since then, a lot more SiC power devices have been launched into the market. Gallium Nitride (GaN) transistors have appeared as another hopeful alternative to replace silicon power devices. All the improvements are related to fundamental material properties of these wide bandgap semiconductors [4, 5]. Although SiC excels in high-temperature applications, the material characteristics of GaN are superior in high efficiency and high frequency applications.

All the theoretical benefits of GaN power devices due to their distinctive material properties will depend on their reliability and robustness validation [6, 7]. The main indicators to evaluate the reliability of these new power devices, related to their sudden death, are the avalanche ruggedness and the short-circuit capability. In this paper, we will focus on the short-circuit behaviour.

Natively, the basic AlGaN/GaN HEMTs has a normally on or depletion mode characteristic, which result critical for appliances with fail-safe requirements. For power electronic applications, it is essential that transistors have a normally off or enhancement-mode characteristic to prevent problems during circuit power up, or for safety fail conditions. For example, if the gate driver fails and its output goes to zero voltage, the HEMT switches to the off-state. Several modifications have been proposed to move the threshold voltage from negative to positive values [8]. As the techniques for make normally off devices can introduce inherent problems on the reliability [9], it is interesting from the point of view of the future applications to test these normally-off devices

under short-circuit. A future promise of the GaN HEMT application is the automotive one, where many power switching devices are used in hybrid electric vehicles (HEVs) and electric vehicles (EVs). To improve the efficiency of “green-cars”, better performance than Si power devices are required for the power devices. GaN power devices are promising candidates for satisfying the requirements [10, 11]. The lateral GaN power device with a blocking voltage of 600 V is suitable for medium power applications at sub systems (compressor in the air conditioner or battery charging system) in HEV and EV. In this application, the HEMT switch must be able to withstand short-circuit (SC) events at DC-bus voltage level around 400 V, long time enough until the protection circuit in the gate driver reacts.

A lot of papers about technology and reliability of Normally-off GaN HEMTs have been published. The SC capability is related to the current robustness of the GaN HEMTs but only few studies have addressed this issue to the author’s knowledge. In [12] a study of an AlGaN/GaN HEMT with SiC substrate estimating the temperature during the SC event is presented, showing that temperature is not responsible of the failure. The estimated temperature is lower than 150 ºC discarding the thermal breakdown, and it is mentioned that the failure mechanism could be due to impact ionization because of the high electric field found in the device.

Later, [13] studies the short-circuit capability of commercial GaN MISHEMTs, finding a good SC capability in some of the tested devices, but others, with apparently the same behaviour, break as soon as 1 μs after the SC event. The paper does not provide any explanation for this behaviour. Recently, in [14, 15] the SC capability of commercial p-GaN and GaN MISHEMTs are analyzed. These studies are focused on explaining what we will call “premature breakdown”, which is the breakdown that occurs around 1μs short-circuit time (t_{sc}). The reason given by the authors is a thermal failure due to a hotspot. Finally, in [16] a gate bias dependence in the SC capability is shown, exhibiting a self-protecting decrease of current and dissipation level during the SC.

Based on all the studies mentioned above and our experimental results reached on commercially available p-GaN and GaN MIS-HEMT, this paper presents a detail SC analysis, showing two different failure mechanisms, one called by the authors “premature breakdown” and the already known thermal breakdown. The premature breakdown is the same for both devices and is related with the high electric field reached on the drain side. Nevertheless, the temperature related breakdown is different for each type of structure. While in the GaN MISHEMT thermal breakdown the drain and source are shorted, in the case of p-GaN HEMT thermal breakdown the failure mechanism is different and is related with a degradation of the gate diode. Technical literature already presents possible reasons of the premature and thermal breakdown as explained later in the paper. No explanation has been found yet for the gate degradation reported.

2. Short-circuit test setup

An experimental setup for the short-circuit tests has been implemented using the circuit depicted in figure 1. This setup enables to implement the short-circuit type I (SC I), that is a direct turn-on of the switch to a short circuit (hard switch fault condition). The setup consists of a low inductance DC voltage source, V_{DD}, having enough capacitance to provide the maximum short-circuit current and still maintaining the DC bus voltage, in parallel with the HEMT. The parasitic inductance (L_{stray}) of the power loop has been experimentally measured using network analyzer Agilent E5061B, showing a value around 60 nH. The drain current (I_D) was measured using a two-step current transformer made of a 1:10 toroid ferrite as a first step, and a 2878 Pearson Electronics current monitor as a second step. This current monitor was selected instead of a coaxial shunt resistor to induce the lowest additional parasitic inductance in the power loop and to withstand the maximum dissipated energy. The gate current (I_G) is also recorded by measuring the voltage drop across an external series gate resistor (R_G) of 20 Ω, (put in series with the input of the gate terminal) using a differential voltage probe (LeCroy HDV3106 120 MHz). On the other hand, the drain to source (V_{DS}) and the gate to source (V_{GS}) voltage have been measured by passive voltage probe (PMK 400 MHz) referenced to the source terminal. The drive circuit used consists in a generic MOSFET gate driver (IXDN609SI), which is controlled by an external arbitrary waveform generator to set the duration of the short circuit. During the test, different bus voltages and external temperatures were applied.

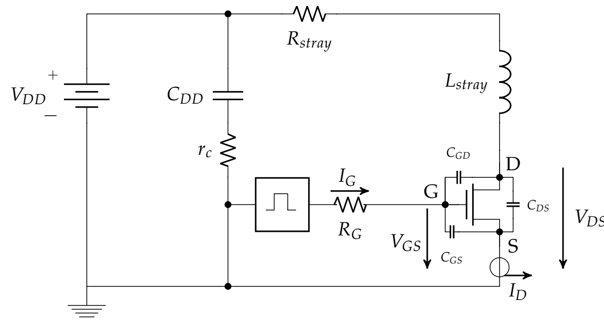

Figure 1. Circuit scheme for SC type I events.

The tested devices are commercially available AlGaN/GaN on Si substrate normally off HEMTs, rated at 600 V. We have selected two different structures: a 600 V p-doped GaN gate (p-GaN) HEMT encapsulated in TO220 (manufactured by Panasonic) and a 650 V GaN Metal-Insulator-Semiconductor HEMT (MISHEMT) encapsulated with embedded die packaging (manufactured by GaN System Inc.). Table 1 summarizes the key parameters of the investigated devices. The gate-to-source voltage level selected for the p-GaN HEMT has been V_{GS}=0 V/4 V and for the GaN MISHEMT V_{GS}=0 V/6 V, with the objective to minimize the conduction losses without increasing the gate losses.

Regarding behaviour of p-GaN HEMT, and according to [17], a recessed p-doped GaN layer on top of the AlGaN/GaN heterostructures acts as a pn-junction gate (like a diode). The p-doped layer depletes the Two-Dimensional Electron Gas (2DEG) channel at zero gate bias. When the V_{GS} applied is higher than the threshold voltage the diode turns on and the device conduction starts. However, the p-GaN devices have a tighter gate voltage limitation, as the gate leakage current would increase what could degrade gate junction reliability or even lead to gate breakdown and device failure [18, 19].

For power applications, it is important to reduce the gate leakage current to minimize the control circuit power consumption in the off state. To achieve noise immunity and wide gate-bias range of operation, low gate leakage is essential for both, reverse and forward gate biasing conditions. To suppress the gate leakage, a metal insulator-semiconductor MISHEMT is often fabricated by inserting a gate dielectric between the Schottky gate and the AlGaN barrier. Nevertheless, recent studies [20] demonstrated that the gate insulator could be a critical element in terms of device reliability. Depending on the deposition method and the material quality, the dielectric/AlGaN interface may have several defects that can induce threshold voltage shift and hysteresis, and even time dependent SC breakdown failure.

Table 1. Parameters of tested devices.

	Symbol	**GaN MIS-HEMT GS66508P**	**p-GaN HEMT PGA26C09DV**
Drain-to-source breakdown voltage	BV_{DSS}	650 V	600 V
Continuous drain current (Tc=25ºC)	I_D	30 A	15 A
Internal Gate resistance (1 MHz)	R_{G-int}	1.1 Ω	4.4 Ω
Drain-to-source ON resistance (Tj=150ºC)	$R_{DS(ON)}$	129 mΩ [a]	150 mΩ [b]
Input Capacitance (1MHz, 400 V)	Ciss	168 pF	259 pF
Total Gate Charge	Q_G	5.8 nC	11 nC

[a] Measured at 9A, [b] Measured at 8A

3. Short circuit behaviour

With the aim of understanding the SC behaviour this work will focus on analyzing the experimental waveforms of the drain current and gate current. In figure 2 is shown a short-circuit event for different drain voltage. Different intervals have been defined for a better understanding.

In the first interval, between t_0 and t_1, the parasitic input capacitance (C_{iss}=C_{GS}+C_{GD}) of the HEMT is charged to enhance the 2DEG channel, so a peak in the gate current is observed. When this peak takes place, the drain current starts to increase, it occurs between t_1 and t_2 in the plateau region. During this interval, the drain current has a slope set by the RL circuit formed mainly by the parasitic inductance and the on-state resistance of the HEMT. This stage ends when the drain current reaches the saturation level $I_{D(sat)}$, at this moment (t_2) the drain current reaches a maximum which then starts to decrease until t_3, time instant at which the DUT is turned off due to the end of the gate pulse.

There are some differences between both devices respect to the shown waveforms. The first one is the shorter time needed by the GaN MISHEMT device to start the conduction (time to reach t_1). This is due to the smaller input capacitance of this device. Later, a different behaviour can be seen between both devices in the maximum $I_{D,max}$ reached during the SC event. In the p-GaN HEMT device, the $I_{D,max}$ showed has a negative dependence with V_{DD}, while the GaN MISHEMT does not show this behaviour, reaching the same value of $I_{D,max}$ independently of V_{DD}. This phenomenon is purely thermal, due to the decrease of the carrier mobility with temperature. In the case of p-GaN HEMT evaluated, the less chip size available involve less time to heat the device, reaching more temperature than GaN MISHEMT. Therefore, for the same short-circuit time the p-GaN HEMT reach enough temperature to cause a decrease of the maximum drain current.

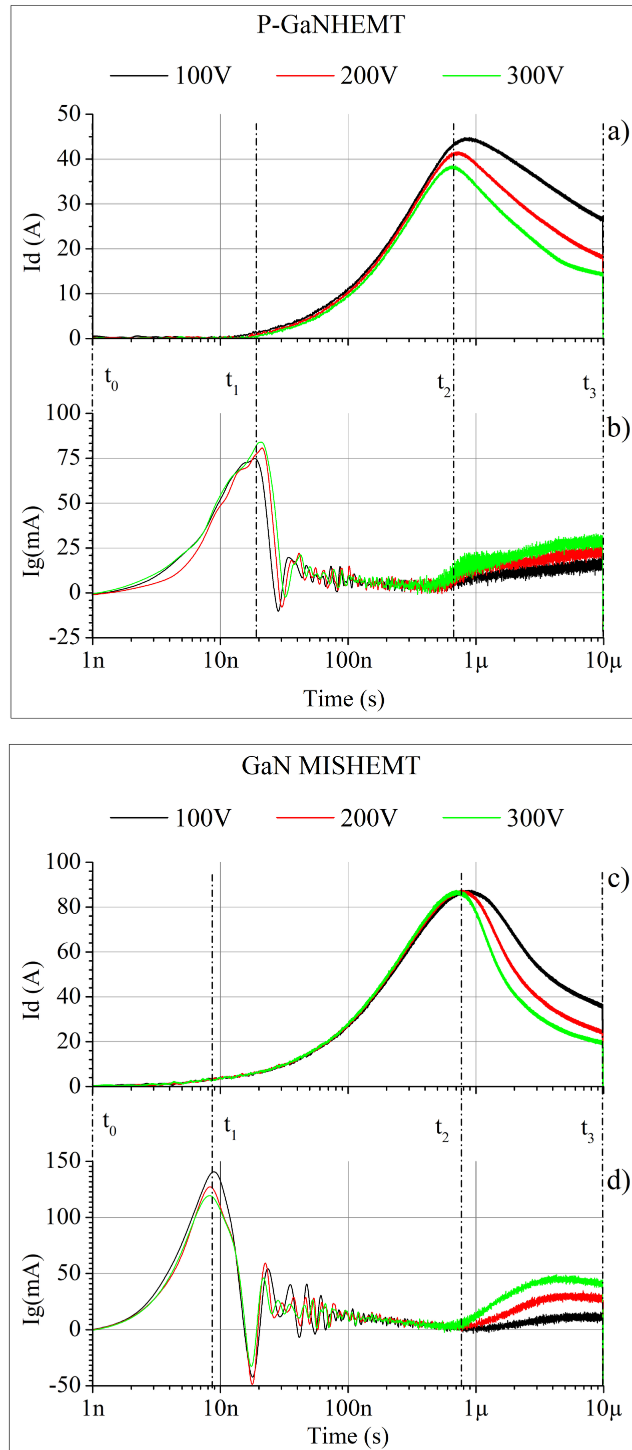

Figure 2. Non-destructive SC experimental waveforms. I_{drain}, I_{gate} at different V_{DD} and at room temperature are shown. (a,b) p-GaN HEMT (c,d) GaN MISHEMT.

On the other hand, from time instant t_2 on, both devices show similar behaviour, reducing their saturation current with time, and also, having a greater current reduction with the increase of the applied V_{DD}. This decay improves the device ruggedness since power dissipation is reduced. This reduction is purely thermal, and the dependence of this current is basically due to the negative dependence of the electro mobility with temperature [21, 22]. Evaluating the GaN transistor temperature during the SC is essential to understanding the limitation of the device. Direct

measurement of the temperature distribution can be done by costly equipment and time-consuming techniques. In particular, micro-Raman spectroscopy has proven to be a powerful technique for measuring temperature profiles with high spatial resolution. Indirect electrical techniques cannot bring any space resolved information but are, simpler and cheaper than direct ones [23]. For this reason, drain current measurement can be used to estimate the channel temperature of the 2DEG channel based on equation 1:

$$I_{SAT}(T) = I_{SAT}(T_0) \cdot \left(\frac{T}{T_0}\right)^{-\alpha} \quad (1)$$

In equation 1, T and T_0 are temperatures in Kelvin units, T_0 is the reference temperature before application of the short-circuit pulse, $I_{SAT}(T_0)$ is the saturation current at temperature T_0 and α is the extracted temperature exponent parameter. In our case we have extracted this parameter measuring the output characteristics (I_D-V_{DS}) at different temperatures with the curve tracer/analyzer Keysight B1505A. The experimental result is shown in figure 3, where the different α parameter for both devices can be seen. In order to know the goodness of fit for the regression model we have obtained the adjusted r-squared for the two HEMT devices.

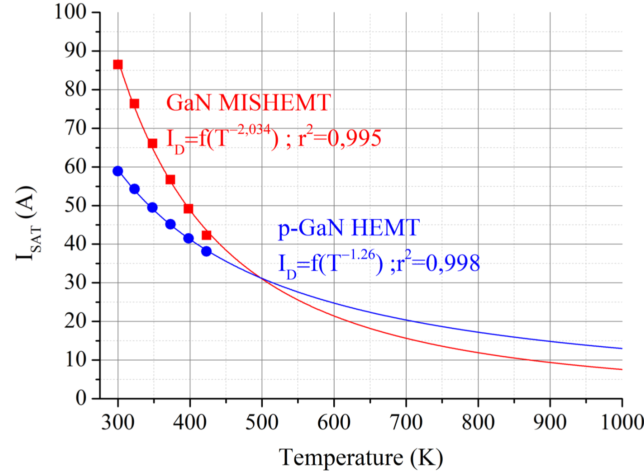

Figure 3. Saturation drain current vs. temperature of p-GaN PGA26C09DV (blue) and GaN MISHEMT GS66508T (red) used to calculate their different α parameter.

It is important to mention that after t_2(figure 2), the gate current I_G increases in both devices. This increase has a positive dependence with bus voltage. To understand if the origin of this increase is due to the V_{DD} increase or the temperature increase in the channel, SC events under different temperatures with a constant V_{DD}=100 V have been done and the results are shown in figure 4.

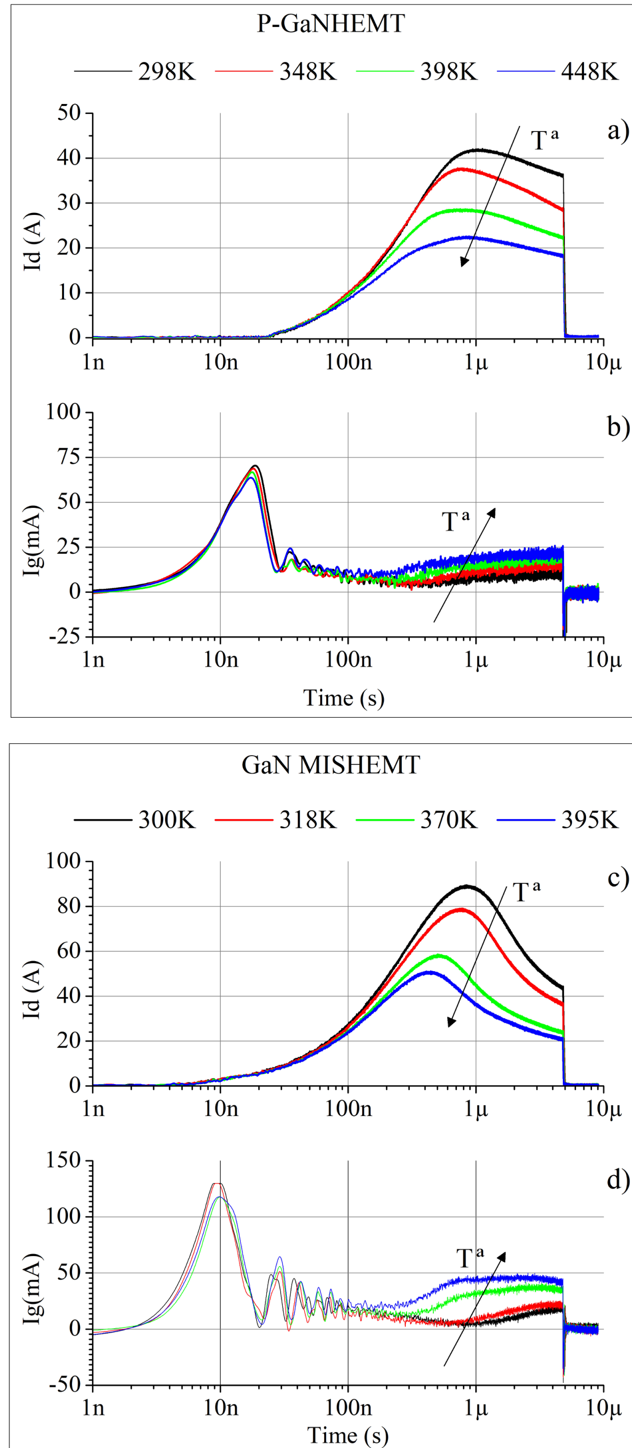

Figure 4 Non-destructive SC experimental waveforms for different temperatures (t_{sc}=5 µs and V_{DD} = 100 V). I_D and I_G (a, b) p-GaN HEMT PGA26C09DV (c, d) GaN MISHEMT GS66508T are shown.

As can be seen, the increase on the gate current during short circuit is proportional to the temperature increase. In [14] a TCAD simulation has been performed for p-GaN HEMT. It shown the internal temperature distribution and a vertical cut of the absolute electric field at its field plate. The heat diffusion from the hotspot generated at the gate and the thermal trend expected for the Schottky contact and the pn-junction, explain the gate current increase. This would induce

also a decrease of the threshold voltage (V_{TH}) with temperature [24]. This assumption agrees with experimental results of V_{TH} negative temperature dependence on these devices, as shown in figure 5. The threshold voltage has been extracted from the transfer characteristics measured under linear regime operation conditions, following the constant current method. This method evaluates the threshold voltage as the value of the gate voltage, corresponding to a given arbitrary constant drain current.

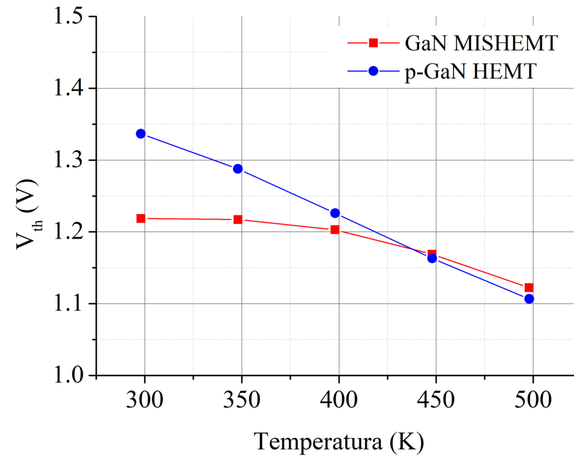

Figure 5. Experimental measurements of V_{TH} with temperature for p-GaN HEMT (PGA26C09DV) and MISHEMT (GS66508T) measured at I_D=10 mA at V_{DS}=1 V.

4. Failure analysis

During the all tests done on both devices, two different breakdown modes have been detected, one induced by the high temperature reached during the SC event, and a second, which is a premature breakdown. Both breakdown mechanisms will be analyzed based on the experimental waveforms.

4.1. Thermal related breakdown

The thermal related breakdown is different in p-GaN HEMTs compared to GaN MISHEMT devices. We will focus first on figure 6, where GaN MISHEMT thermal breakdown is shown. As can be seen in these waveforms, at the time of breakdown (around t_{sc}=270 µs for V_{DD}=400 V), a high drain current increase takes place. This breakdown induces a short-circuit between drain and source, and the energy of the input capacitor bank, is transferred to the device, in an uncontrolled way.

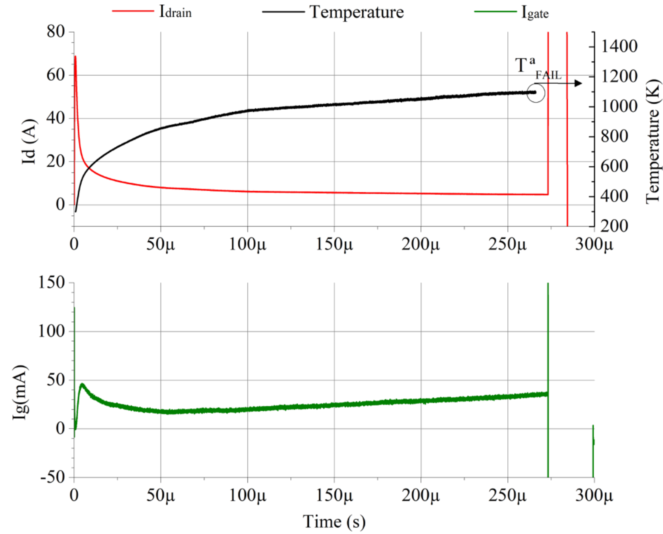

Figure 6. Thermal breakdown experimental waveforms at 270 µs for V_{DD}= 400 V- GS66508T GaN MISHEMT.

The estimated mean temperature at breakdown in the 2DEG channel is around 1100 K, near the intrinsic temperature of gallium nitride (1667 K). At this range of temperature, the semiconductor becomes intrinsic, with the reduction of two-dimensional electron gas (2DEG) mobility and carrier velocity, and therefore due to its resistive behaviour, the failure is thermally induced. Also, thermomechanical stress induced by the high temperature may appear as explained in [23]. Other authors have demonstrated that thermal breakdown in a similar temperature range may happen in the field plates, which match with our temperature estimation [25]. This thermal failure causes a short-circuit between drain and source, which ends up causing the burn out of the device due to the high energy dissipated.

On the other hand, the p-GaN HEMT breakdown is different from the GaN MISHEMT. The breakdown waveforms are also different and, in this case, no SC between drain and source appears. As shown in figure 7, the breakdown signature is a sudden drop in the drain current, that takes place at 61 µs for V_{DD} = 400 V, due to the sudden increase of the gate current.

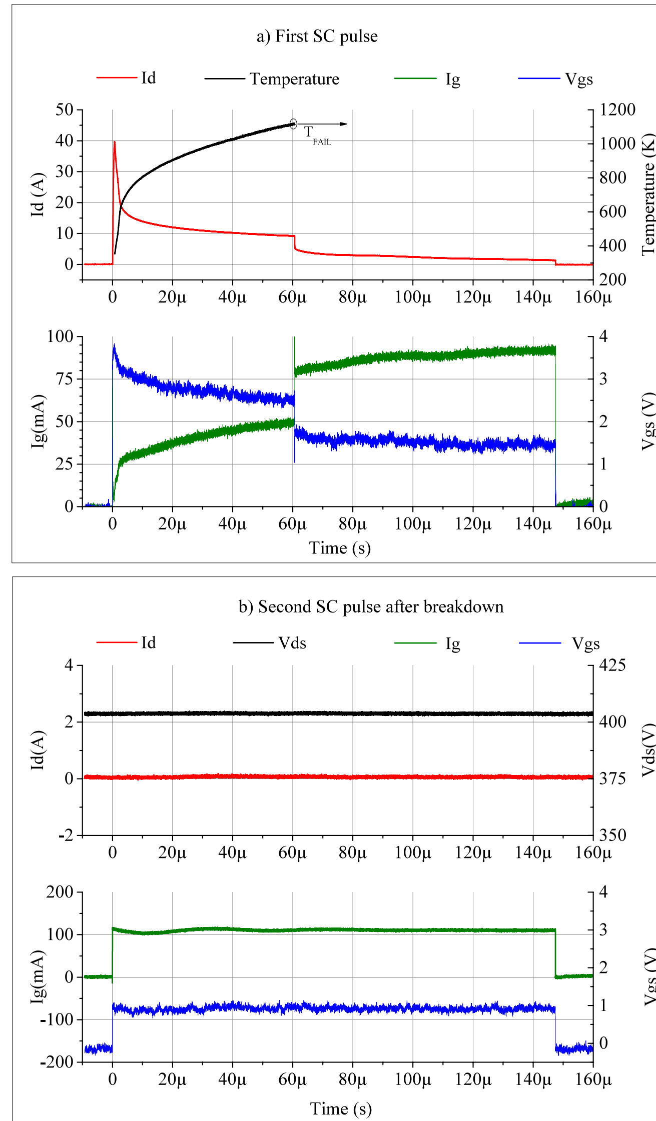

Figure 7. Temperature related breakdown experimental waveforms for p-GaN HEMT PGA26C09DV (t_{sc}=150 µs and V_{DD} = 400 V). a) Waveforms at the first SC pulse b) Waveforms on the second SC pulse after breakdown.

Based on the figure 7 waveforms, the breakdown is due to a degradation of the pn junction or the Schottky contact presents between gate and source edges, which causes a high increase in the gate current. This increase in gate current, which passes through R_G induces a drop in V_{GS}, resulting in the consequent reduction of the drain current. This breakdown mode results in a loss of gate control for the p-GaN device, due to the degradation of the gate current characteristic. The temperature estimated at breakdown is the same for both devices, around 1100 K, however; in this case, the breakdown is related to the gate region. To demonstrate that the device was broken in the gate region, another second pulse was applied. Figure 7b shown the behavior during the second SC pulse. Is appreciated how the gate leakage current was increased hugely, with the consequent reduction in the gate voltage inhibiting gate control and therefore, there is no drain current through the device during the pulse of V_{GS}.

4.2. Premature breakdown

The other type of breakdown, shown by both devices in SC, is what we have called premature breakdown. This type of breakdown is not related with the maximum temperature reached, due to the low temperature estimated at the breakdown instant: 380 K in the case of p-GaN HEMT

and 330 K in the case of the GaN MISHEMT. Waveforms and temperature estimation for this breakdown are showed in figure 8.

In both devices, this breakdown takes place between drain and gate. This breakdown causes the destruction of the device, transferring the capacitor bank energy to the device.

Comparing the gate current in figure 8 and figure 2 for both devices, there are no changes in the dynamic behaviour that could be used to predict the failure event. Therefore, there is no electrical evidence to predict the premature failure. This type of breakdown can be explained in terms of hot-electron effect. During the SC event, the device suffers a large I_{DS} with a large V_{DS} (semi-ON state), the electroluminescence analysis done in [26] with a similar p-GaN device explains this hot electron effect, which causes the generation of traps at the surface that can shift the electric field to the drain edge making it increase, and then, when the electric field at the drain edge exceeds the critical electric field for the device, the device breaks [27].

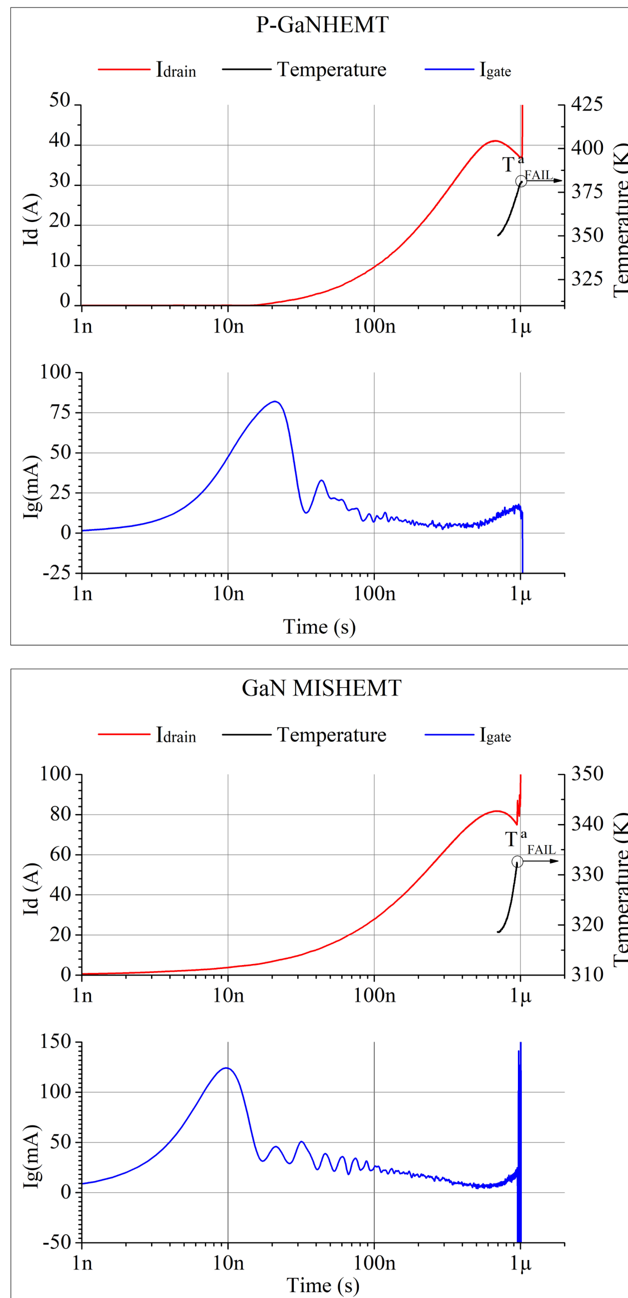

Figure 8. Premature breakdown experimental waveforms at V_{DD}= 400 V for p-GaN HEMT PGA26C09DV and GaN MIS-HEMT GS66508T.

5. Discussion

Based on the two types of breakdown showed in section 4, table 2 shows the time to breakdown of both devices analyzed with two different bus voltages, discriminating the type of breakdown. Table 2 evidence that premature breakdown times are much shorter than the thermal related breakdown for all the voltages. This means that the actual critical point of this device is the premature breakdown which is a breakdown related with the high electric field generated and not due to the thermal effect that has a large time constant. Therefore, the way to improve the capability of SC of these devices could be focusing in increasing the electric field they support. It is also important to mention that premature breakdown only occurs in p-GaN HEMT for drain voltages of 400 V and higher, while in GaN MISHEMT it occurs already at drain voltages of 350 V. This could be due to the influence of the metal insulator effect to support high electrical field. The use of a MIS-type gate stack in the GaN MISHEMT devices, result in a minimization of the gate leakage and allows positive gate bias without gate current injection, unlike the p-GaN MISHEMT. However, in the MIS-type gate the main drawback is the threshold voltage instability due to the interface/border traps in the insulator, and the time-dependent dielectric breakdown of the very thin insulator. These failure mechanisms are induced by high electric field and for the MISHEMT depend on the chosen gate dielectric material and on the related deposition techniques [9].

The SC event represents the most hard-switching condition for a power transistor. In fact, during the ON transition the hard-switching load-line trajectories combine a very high voltage and high current levels overlapping. This event could generate highly energetic electrons (hot-electrons), which can promote long-term reliability issues and also instantaneous charge-trapping effects, and if the hot-electrons density generated is enough, permanent degradation mechanism can occur. Some of the hot electrons can be trapped at the AlGaN surface, thereby the electric field distribution is modified and the peak electric field moves from the gate edge to the drain edge.

On the other hand, the time to breakdown of the thermal breakdown has a negative dependence on the applied bus voltage, reducing the time to breakdown when the bus voltage is increased. This is basically due to the higher dissipation with higher bus voltage, which reduces the time needed to heat up the device.

Finally, a special consideration has been shown in the thermal breakdown, that is completely different for p-GaN HEMT and MISHEMT. While in GaN MISHEMT a short-circuit between drain and source occurs, in the case of p-GaN HEMT the breakdown occurs at the gate, without having a short-circuit between drain and source. This behaviour is also confirmed by the measured times. While premature breakdown occurs around the same times for both devices, the thermal breakdown occurs much later, although earlier for p-GaN HEMT than for GaN MIS-HEMT.

Table 2. Extracted breakdown parameters for the tested devices.

		GaN MISHEMT PN: GS66508T		p-GaN HEMT PN: PGA26C09DV	
Breakdown type		Premature	Thermal	Premature	Thermal
V_{DD} 350 V	t_{sc} (s)	2.4 μ	350 μ	-	70 μ
	$E_{SC,crit}$(J)	50 m	980 m	-	315 m
V_{DD} 400 V	t_{sc} (s)	1 μ	270 μ	1 μ	60 μ
	$E_{SC,crit}$(J)	25 m	800 m	10 m	290

6. Conclusion

The SC capability of commercial 600 V p-GaN HEMTs and 650 V GaN MISHEMTs has been tested and analyzed. A comparison between both devices has been made based on experimental results.

The temperature estimation for the 2DEG channel allows to concluding that different breakdown mechanisms are involved in both devices. One is the temperature related breakdown, which is different for both devices. While GaN MISHEMT breakdown involves a SC in the device, in the

case of p-GaN HEMT the temperature breakdown induces a gate breakdown, disabling gate control for the device.
Nevertheless, the main problem is that both devices can suffer a not temperature related breakdown, called as premature breakdown, because it occurs very soon during the short-circuit event. This type of failure is a bottleneck at this moment for normally-off commercial GaN HEMT devices because it reduces considerably their robustness. So, to improve the short-circuit capability of GaN HEMTs it is necessary to focus on improving the electric field that they are able to withstand more than focusing on limiting the saturation drain current as could be expected. The power dissipation is not the most critical point, since the thermal breakdown which is caused by power dissipation takes place, in the worst-case, around 50 μs after the SC event for the case of V_{DD} = 400 V. Time enough for the intervention of the protection circuits to protect the device. In any case the improvements regarding the extraction of the heat out the device can help to overcome the local thermal breakdown.

Acknowledgment

This work was partially funded by the Spanish MINECO and FEDER grant ESP2015-68117-C2-1-R

References

[1] ECPE Position Paper on Next Generation Power Electronics based on Wide Bandgap Devices - Challenges and Opportunities for Europe. [Online]. Available: http://www.ecpe.org/roadmaps-strategy-papers/strategy-papersAnother reference.
[2] Chow T P 2014 Progress in high voltage SiC and GaN power switching devices, Mater. Sci. Forum, vols. 778–780, pp. 1077–1082.
[3] Chow T P 2015 Wide bandgap semiconductor power devices for energy efficient systems in *Proc. IEEE Workshop Wide Bandgap Power Dev. Appl.* (*WiPDA*) 402–405.
[4] Chowdhury S et al 2014 Comparison of 600V Si, SiC and GaN power devices *Mater. Sci. Forum* 778–780 971–974.
[5] Millán J, Godignon P, Perpiñà X, Pérez-Tomás A, and Rebollo J 2014 A survey of wide bandgap power semiconductor devices, *IEEE Trans. Power Electron.* 29 2155–2163.
[6] Meneghesso G et al 2016 Reliability and parasitic issues in GaN-based power HEMTs: a review *Semiconductor Science and Technology* 31 093004.
[7] Wuerfl J et al 2011 Reliability issues of GaN based high voltage power devices *Microelectronics Reliability* 52 1710-1716
[8] Jones E A, Wang F and Ozpineci B 2014 Application-based review of GaN HFETs *IEEE 2nd Workshop on Wide Bandgap Power Devices and Applications* pp 24-29.
[9] Zanoni E et al 2015 Reliability and failure physics of GaN HEMT, MIS-HEMT and p-gate HEMTs for power switching applications: Parasitic effects and degradation due to deep level effects and time-dependent breakdown phenomena, *IEEE 3rd Workshop on Wide Bandgap Power Devices and Applications (WiPDA)* pp. 75-80
[10] Nishikawa K 2013 GaN for automotive applications *IEEE Bipolar/BiCMOS Circuits and Technology Meeting (BCTM)* 143-150.
[11] Su M etl al 2013 Prospects for the application of GaN power devices in hybrid electric vehicle drive systems Semicon. Sci. and technol. 28 074012.
[12] Huang X et al 2014 Experimental study of 650V AlGaN/GaN HEMT short-circuit safe operating area (SCSOA) *IEEE 26th International Symposium on Power Semiconductor Devices & IC's (ISPSD)* 273-276.
[13] Landel M et al 2016 Experimental study of the short-circuit robustness of 600V E-mode GaN transistors *Microelectronics Reliability* 64 560-565
[14] Fernández M et al 2017 P-GaN HEMTs Drain and Gate Current Analysis Under Short-Circuit, IEEE *Electron Device Letters* 38 505-508.
[15] Fernández M et al. 2017 Short-Circuit Study in Medium Voltage GaN Cascodes p-GaN

HEMTs and GaN MISHEMTs in *IEEE Transactions on Industrial Electronics* 99 1-1.
[16] Oeder T, Castellazzi A and Pfost M 2017 Experimental study of the short-circuit performance for a 600V normally-off p-gate GaN HEMT *29th International Symposium on Power Semiconductor Devices and IC's (ISPSD)* Sapporo 211-214.
[17] Tanaka K, et al 2015 Suppression of current collapse by hole injection from drain in a normally- off GaN-based hybrid-drain-embedded gate injection transistor *Appl. Phys. Lett.* 107 10 163502-1–163502-4.
[18] Meneghini M et al 2016 Gate Stability of GaN-Based HEMTs with P-Type Gate Electronics 5 14
[19] Lee F et al 2015 Impact of Gate Metal on the Performance of p-GaN/AlGaN/GaN High Electron Mobility Transistors *IEEE Electron Dev. Lett.* vol. 36 3 232-234.
[20] Yatabe Z et al 2016 Insulated gate and surface passivation structures for GaN-based power transistors *J. Phys. D: Appl. Phys.* 49393001
[21] Alim M. A et al 2015 Thermal characterization of DC and small-signal parameters of 150 nm and 250 nm gate-length AlGaN/GaN HEMTs grown on a SiC substrate Semicon. *Sci. and technol.* 30, 125005
[22] Giovanni C. et al 2011 Investigation on the thermal behavior of microwave GaN HEMTs. *Solid-State Electronics* Volume 64 Issue 1 Pages 28-33.
[23] Nagahisa T et. al. 2016 Robust 600 V GaN high electron mobility transistor technology on GaN-on-Si with 400 V, 5 μs load-short-circuit withstand capability *Jpn. J. App. Phys.* 55 04EG01.
[24] Li X et al 2016 Charge trapping related channel modulation instability in P-GaN gate HEMTs *Microelectronics Reliability* 65 35-40.
[25] Zhou L et al 2017 Investigation on Failure Mechanisms of GaN HEMT Caused by High-Power Microwave (HPM) Pulses in *IEEE Trans. on Electromagnetic Compatibility* 59 3 902-909.
[26] Meneghini M et al 2012 Time and Field-Dependent Trapping in GaN-Based Enhancement-Mode Transistors With p-Gate *IEEE Electron Dev. Letters* 33 375-377.
[27] Tanaka K et al 2017 Reliability of hybrid-drain-embedded gate injection transistor *IEEE International Reliability Physics Symposium (IRPS)* Monterey CA 4B-2.1-4B-2.10.